Inflammatory Demyelinating Disease Mimicking Malignant Glioma

Toshiaki Hayashi, MD[1]; Toshihiro Kumabe, MD[1]; Hidefumi Jokura, MD[1]; Kazuo Fujihara, MD[2]; Yusei Shiga, MD[2]; Mika Watanabe, MD[3]; Shu-ichi Higano, MD[4]; and Reizo Shirane, MD[1]

[1]Department of Neurosurgery, Tohoku University Graduate School of Medicine, Sendai, Japan; [2]Department of Neurology, Tohoku University Graduate School of Medicine, Sendai, Japan; [3]Department of Pathology, Tohoku University Graduate School of Medicine, Sendai, Japan; and [4]Department of Radiology, Tohoku University Graduate School of Medicine, Sendai, Japan

The differential diagnosis between inflammatory demyelinating disease and malignant glioma is difficult based only on neuroimaging methods. **Methods:** Four patients with inflammatory demyelinating disease who presented with clinical and neuroimaging findings strongly suggestive of malignant glioma were examined. **Results:** MRI showed a mass lesion with prolonged T1 and T2 values and gadolinium enhancement in all cases. Proton MR spectroscopy and ^{201}Tl SPECT showed findings supportive of the diagnosis of malignant glioma in all cases. However, surgical biopsy revealed inflammatory demyelinating disease. After the diagnosis, 2 patients were treated by steroid administration and 2 were just observed. The gadolinium enhancement of all lesions decreased and finally disappeared. **Conclusion:** Such cases illustrate the importance of considering a demyelinating lesion in the differential diagnosis of a mass lesion. The difficulties encountered in establishing the correct diagnosis of inflammatory disease are related to the variations in the radiologic appearance, which require exclusion of gliomas or other brain tumors by surgical biopsy before the therapeutic strategy can be selected.

Key Words: inflammatory demyelinating disease; malignant glioma; proton magnetic resonance spectroscopy; ^{201}Tl SPECT

J Nucl Med 2003; 44:565–569

Inflammatory demyelinating diseases, such as multiple sclerosis and encephalomyelitis, occasionally present as a mass lesion that is indistinguishable clinically and radiologically from a brain tumor. MRI has demonstrated several cases of inflammatory demyelinating disease mimicking brain tumor (*1–7*). MRI of demyelinating disease is characterized by prolongation of the T1 and T2 values, probably due to inflammatory changes such as focal softening of the brain tissue with loss of myelin sheaths and glial proliferation, meningeal and perivascular infiltration of lymphocytes and plasma cells, and consecutive edema. Contrast enhancement is correlated with active demyelination in the acute stage, indicating breakdown of the blood–brain barrier (*3,8,9*). MRI of demyelinating disease generally shows multiple plaques with enhancement and absence of mass effect, but associated mass effect and ring enhancement are known (*1,2,4*).

We describe 4 cases of inflammatory demyelinating disease that presented as a mass lesion mimicking malignant glioma. MRI, proton MR spectroscopy (^{1}H MRS), and ^{201}Tl SPECT findings were all suggestive of glioma.

MATERIALS AND METHODS

Patients

Patient 1. A 20-y-old man developed left hemiparesis 2 wk before admission. MRI revealed a mass lesion in the right basal ganglia, which was hypointense on the T1-weighted images and hyperintense on the T2-weighted images with heterogeneous enhancement after gadolinium-diethylenetriaminepentaacetic acid (Gd-DTPA) administration (Fig. 1A). The ^{1}H MRS spectrum was noisy, but increased choline (Cho) and decreased *N*-acetylaspartate (NAA) peaks were evident (Fig. 1B). ^{201}Tl SPECT showed high uptake in the lesion on both early and delayed images (Fig. 1C). Analysis of the cerebrospinal fluid (CSF) detected no obvious oligoclonal band or pleocytosis and no myelin-basic protein. The total protein and IgG indices showed no specific indications. These findings strongly suggested that the lesion was a malignant glioma. Stereotactic biopsy was performed under MRI guidance. Histologic examination of the tumor specimen revealed that the lesion consisted of infiltrated inflammatory cells, mainly lymphocytes and gliosis (Fig. 1D). Demyelination with foamy macrophages was also present. No bizarre or pleomorphic astroglial nuclei suggestive of malignant glioma were seen. The histologic diagnosis was inflammatory demyelinating disease. Follow-up MRI showed remission of the lesion without medication. The enhanced component of the lesion decreased in size and finally disappeared. ^{201}Tl SPECT scans showed no uptake on both early and delayed images. The left hemiparesis began to improve. He has done well without relapse for 24 mo.

Patient 2. A 43-y-old man was admitted to our neurosurgical department complaining of generalized convulsion. Neurologic examination revealed no focal neurologic deficit except left homonymous hemianopsia. MRI revealed a mass lesion in the right occipital region that was hypointense on the T1-weighted images

Received Jul. 8, 2002; revision accepted Sep. 27, 2002.

For correspondence or reprints contact: Toshihiro Kumabe, MD, Department of Neurosurgery, Tohoku University Graduate School of Medicine, 1-1 Seiryo-machi, Aoba-ku, Sendai, 980-8574 Japan.

E-mail: kuma@nsg.med.tohoku.ac.jp

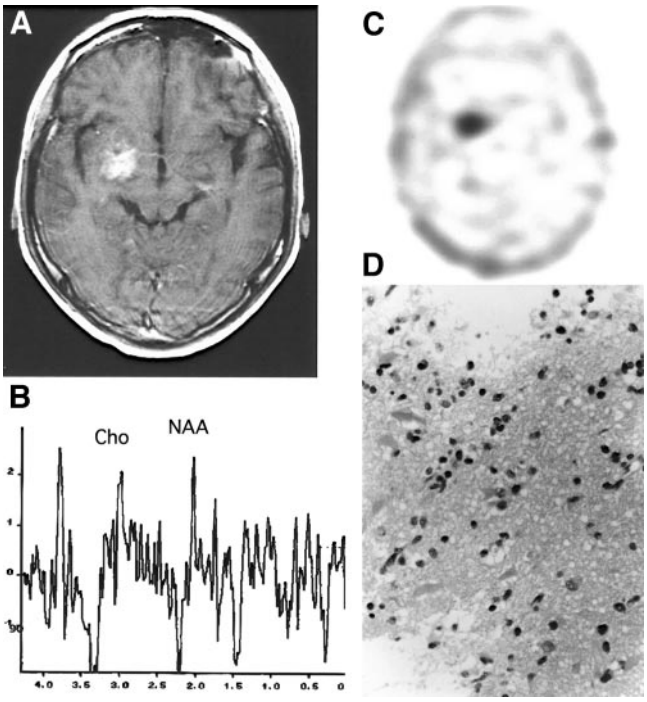

FIGURE 1. Patient 1. (A) T1-weighted MR image with gadolinium shows heterogeneously enhanced mass lesion with minimal mass effect in right basal ganglia. (B) ^{1}H MRS spectrum shows increased choline (Cho) and decreased *N*-acetylaspartate (NAA) peaks. No lactate peak is clearly shown because of noise. (C) ^{201}Tl SPECT scan shows high uptake of tracer in lesion (early image). (D) Photomicrograph of specimen shows infiltration of inflammatory cells mainly consisting of lymphocytes and gliosis. Demyelination with foamy macrophages and hypertrophic astroglia are also present. (Hematoxylin–eosin, ×200)

and hyperintense on the T2-weighted images, with heterogeneous enhancement after Gd-DTPA administration (Fig. 2A). CSF studies showed no specific indications. ^{1}H MRS showed increased Cho and decreased NAA peaks and a positive lactate/lipids peak (Fig. 2B). ^{201}Tl SPECT showed high uptake in the lesion (Fig. 2C). MRI-guided stereotactic biopsy was performed under a presumptive diagnosis of malignant glioma. Histologic examination revealed that the lesion consisted of infiltrated inflammatory cells and gliosis (Fig. 2D). The histologic diagnosis was inflammatory demyelinating disease. Follow-up MRI showed remission of the lesion without medication. The enhanced component of the lesion decreased and finally disappeared. ^{201}Tl SPECT showed no uptake in the lesion on both early and delayed images. He has done well without relapse for 24 mo.

Patient 3. A 47-y-old man developed right hemiparesis, including the right side of the face, 2 mo before admission. MRI revealed a mass lesion in the left deep white matter that was hypointense on the T1-weighted images and hyperintense on the T2-weighted images, with ring-like enhancement after Gd-DTPA administration (Fig. 3A). CSF studies showed no specific indications. ^{1}H MRS demonstrated increased Cho and decreased NAA peaks (Fig. 3B). ^{201}Tl SPECT showed high uptake in the lesion on both early and delayed images (Fig. 3C). MRI-guided stereotactic biopsy was performed under the presumptive diagnosis of malignant glioma. Histologic examination revealed that the lesion was inflammatory demyelinating disease (Fig. 3D). He was given high-dose steroid treatment (pulse therapy and sequential oral treatment of prednisone, 60 mg/d). The lesion decreased and finally disappeared. ^{201}Tl SPECT scans showed no uptake on both early and delayed images. He has done well without relapse for 41 mo.

Patient 4. A 63-y-old man developed left hemiparesis 1 mo before admission. MRI revealed a mass lesion in the right frontal lobe that was hypointense on the T1-weighted images and hyperintense on the T2-weighted images, with heterogeneous enhancement after Gd-DTPA administration (Fig. 4A). ^{1}H MRS showed increased Cho and decreased NAA peaks and a positive lactate/lipids peak (Fig. 4B) ^{201}Tl SPECT showed high uptake in the lesion on both early and delayed images (Fig. 4C). Analysis of CSF showed no specific indications. Open biopsy was performed under a presumptive diagnosis of malignant glioma. Histologic examination of the tumor specimen revealed that the lesion was inflammatory demyelinating disease (Fig. 4D). Treatment was started with intravenous betamethasone administration (4 mg/d for 5 d). His left hemiparesis began to improve. The heterogeneous enhancement of the lesion decreased and finally disappeared. ^{201}Tl SPECT showed no uptake on both early and delayed images. He has done well without relapse for 27 mo.

^{201}Tl SPECT

^{201}Tl SPECT imaging was performed on each patient. ^{201}Tl chloride (111 MBq [3 mCi]) was injected, and brain images were obtained (Siemens MULTI SPECT3 scanner [a triple-head gamma camera equipped with a fanbeam collimater]; Siemens Gammasonics, Hoffman Estates, IL, connected to an ICON P workstation) at 15 min (early images) and 3 h (delayed images) after injection.

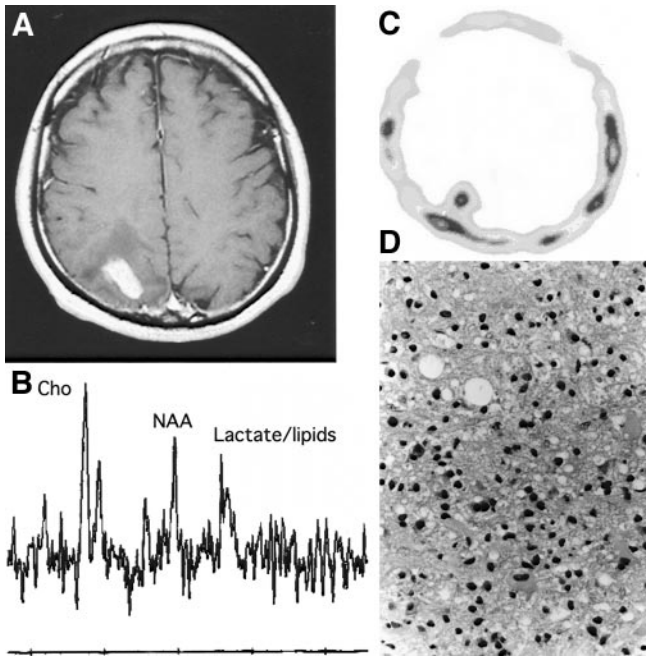

FIGURE 2. Patient 2. (A) T1-weighted MR image with gadolinium shows enhanced mass lesion in right occipital region with perifocal edema. (B) ^{1}H MRS spectrum shows increased Cho and decreased NAA peaks. Lactate peak is also shown. (C) ^{201}Tl SPECT scan shows high uptake of tracer in lesion (early image). (D) Photomicrograph of specimen shows infiltrated inflammatory cells and gliosis. Demyelination with foamy macrophages is also present. (Hematoxylin–eosin, ×200)

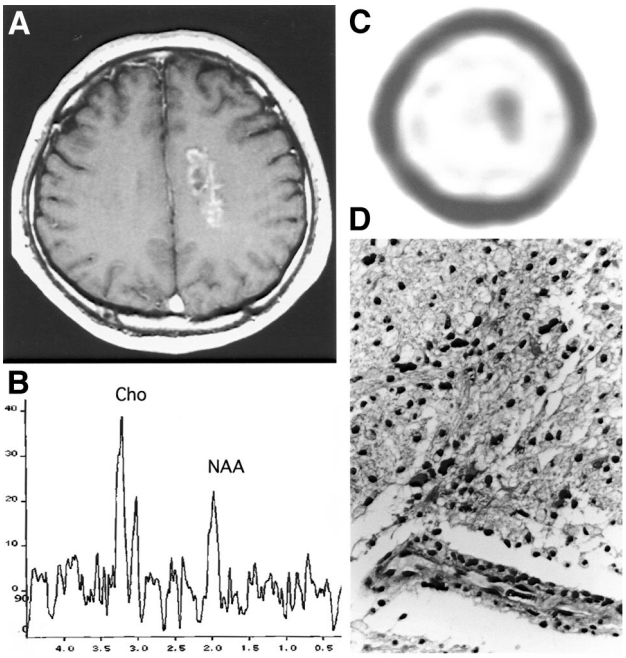

FIGURE 3. Patient 3. (A) T1-weighted MR image with gadolinium shows mass lesion with ring enhancement in left paraventricular white matter. (B) ^{1}H MRS spectrum shows increased Cho and decreased NAA peaks. (C) ^{201}Tl SPECT scan shows high uptake of tracer in lesion (early image). (D) Photomicrograph of specimen shows focal collections of inflammatory cells and foamy macrophages surrounding blood vessels. No atypical nuclear cells are seen. (Hematoxylin–eosin, ×200)

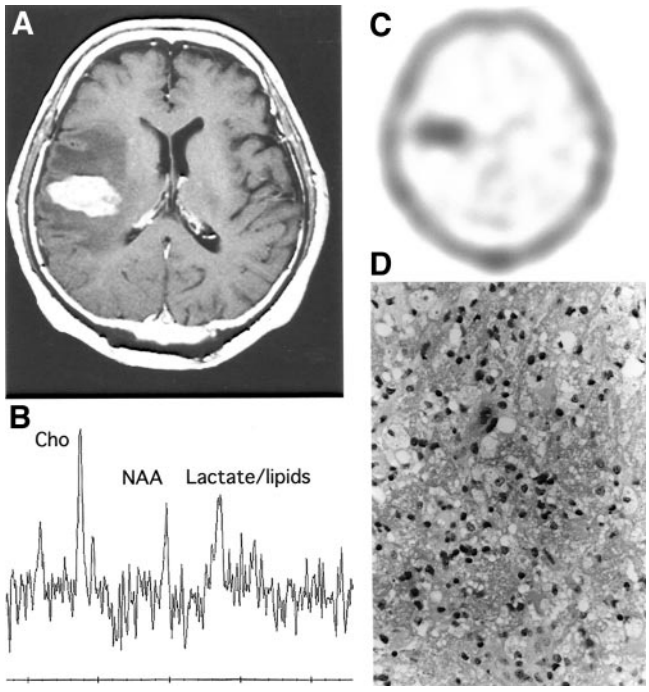

FIGURE 4. Patient 4. (A) T1-weighted MR image with gadolinium shows enhanced mass lesion in right frontal region with perifocal edema. (B) ^{1}H MRS spectrum shows increased Cho and decreased NAA peaks. Lactate/lipids peak is also shown. (C) ^{201}Tl SPECT scan shows high uptake of tracer in lesion (early image). (D) Photomicrograph of specimen shows infiltrated inflammatory cells and gliosis. Demyelination with foamy macrophages is also present. (Hematoxylin–eosin, ×200)

Data were collected from 90 views in a 64 × 64 matrix with an acquisition time of 20 min for the early scan and 25 min for the delayed scan. A Butterworth filter was used. The SPECT images were constructed in the transverse plane to facilitate comparison with the MR images. Regions of interest (ROIs) were drawn on the slice with the greatest tumor activity. Each ROI was square (2 × 2 pixels). Using the system's ROI program, the same ROI could be easily moved to the area of the contralateral region. The ^{201}Tl index was defined as the fraction of the mean counts per pixel in the corresponding contralateral region. The early and delayed ^{201}Tl indices, TIE and TID, respectively, were calculated as the ratios of tumor to normal brain tissue uptake. The retained index (RI) was calculated as (TIE − TID)/TIE.

^{1}H MRS

^{1}H MRS was also performed on each patient. Single-voxel point-resolved spectroscopy used a 1.5-T system and a standard head coil for imaging with spectral width, 2,500 Hz; 2,048 data points; repetition time, 2,000 ms; echo time, 272 ms; and averaged over 128 acquisitions. The size and location of the voxel of interest were carefully adjusted to include the most homogeneous or representative part of the tumor. Spectroscopic measurements were performed before administration of gadolinium. Shimming and water suppression were analyzed with automatic software (SA/GE; General Electric Medical Systems, Milwaukee, WI). The relative peak ratios of NAA, creatine phosphate (Cre), and Cho were also analyzed.

These studies were performed as routine clinical examination. Informed consent was obtained from the each patient before the studies.

RESULTS

^{201}Tl SPECT revealed high uptake in all lesions on both early and delayed scans. The TIE and TID were 2.85 and 3.35 in patient 1, 2.76 and 2.29 in patient 3, and 2.94 and 2.60 in patient 4, respectively. The TIE of patient 2 was 3.73 (TID of patient 2 was not analyzed) (Table 1). The RIs were −1.75 in patient 1, 0.17 in patient 3, and 0.12 in patient 4, respectively. A previous ^{201}Tl SPECT study of 54 patients with gliomas in our neurosurgical department showed that the thresholds of TID were 1.5 between grade 2 and grade 3 glioma and 2.2 between grade 3 and grade 4 glioma. The RIs were 0.02 ± 0.26 in grade 2 astrocytoma, 0.042 ± 0.23

TABLE 1
^{201}Tl Indices and Relative Peak Ratios

Patient no.	TIE	TID	RI	NAA/Cre	Cho/Cre
1	2.85	3.35	−1.75	NA	NA
2	3.73	NA	NA	1.26	1.90
3	2.76	2.29	0.17	1.17	2.11
4	2.94	2.60	0.12	2.13	4.6

NA = not available.

TABLE 2
^{201}Tl Indices in 54 Astrocytomas

Grade	*n*	TIE	TID	RI
2	14	1.38 ± 0.24	1.08 ± 0.18	0.002 ± 0.26
3	19	2.18 ± 2.37	1.88 ± 1.39	0.042 ± 0.23
4	21	4.24 ± 2.40	3.25 ± 1.43	0.15 ± 0.25

Data are expressed as mean ± SD.

in grade 3 astrocytoma, and 0.154 in grade 4 astrocytoma (Table 2).

^{1}H MRS demonstrated increased Cho and decreased NAA peaks in all 4 patients. The lactate/lipids peak was positive in patients 2 and 4. The Cho/Cre and NAA/Cre ratios were 1.90 and 1.26 in patient 2, 2.11 and 1.17 in patient 3, and 4.6 and 2.13 in patient 4, respectively (Table 1). The semiquantitative value of the parameters in patient 1 was not evaluated because of the low signal-to-noise ratio. A previous ^{1}H MRS study showed that the normal values (mean ± 2 SD) of Cho/Cre and NAA/Cre are 0.54 ± 0.10 and 0.42 ± 0.07 (*14*).

DISCUSSION

Initial MRI of our 4 patients showed a solitary mass lesion with mass effect. ^{1}H MRS and ^{201}Tl SPECT were performed to determine the biologic activity. ^{1}H MRS can determine the intensity ratios of certain brain metabolites, thus providing information on the course of neuronal damage (*4,6,7,9–12*). In our patients, the values of NAA/Cre and Cho/Cre indicated the presence of decreased NAA and increased Cho levels. MRS is useful for the diagnosis of demyelinating disease, monitoring its progression, and evaluating the response to treatment (*4,6–8,10,12,13*). Decreased NAA/Cre ratios due to neuronal or axonal loss concomitant with increased Cho levels corresponding to glial proliferation occur in the plaques of patients with clinically stable or chronically active multiple sclerosis and inflammatory disease. A higher Cho/Cre ratio may reflect breakdown of the myelin membrane phospholipids. Increased lactate levels are associated with inflammation. Macrophages are a possible source of increased lactate because of the high lactate production. However, the ^{1}H MRS characteristics of malignant glioma include decreased NAA and increased Cho and lactate levels, so these findings allow inflammatory demyelinating disease to mimic malignant glioma (*6,12,14*). Accurate diagnosis of multiple sclerosis without biopsy may be possible by using pattern recognition analysis in ^{1}H MRS (*6*), but further study with a larger number of cases is needed to confirm this important possibility.

^{201}Tl SPECT is useful for the evaluation of brain tumors and determination of the malignancy grade of glial tumors (*12,15–20*). The ^{201}Tl uptake observed on early images is believed to depend on blood–brain barrier dysfunction and increased regional blood flow. The ^{201}Tl uptake observed on delayed images may depend on active transport by the membrane Na^{+}-K^{+} adenosine triphosphatase pump of the tumor cells. The K^{+} analog ^{201}Tl is directly taken up into malignant tumor cells (*17*). The ^{201}Tl delay index is significantly higher in high-grade gliomas (World Health Organization [WHO] grades 3–4) than in low-grade gliomas (WHO grades 1–2), so it may be useful for the evaluation of both grade and malignancy of brain tumors (*12,15–20*). All of our patients showed high uptake on both early and delayed images, which indicated high-grade gliomas. The high RI value in patients 3 and 4 also was suggestive of high-grade glioma. A high TIE may also be caused by blood–brain barrier dysfunction due to inflammation. A high TID could be caused by the proliferation of inflammatory cells due to active inflammation, which disappeared in our patients at follow-up. Therefore, the inflammatory process can also cause high uptake of ^{201}Tl, although the process is different than that in malignant tumors, which disappears at the chronic stage (*17–19*). Even the RI could not differentiate inflammatory disease from malignant glioma.

The differential diagnosis between inflammatory disease and malignant glioma is difficult based only on neuroimaging methods. The diagnosis can be confirmed only by the subsequent relapse of the symptoms and the changes detected by the imaging study. Therefore, surgical biopsy and histologic studies are necessary to establish the correct diagnosis. Surgical biopsy specimens of inflammatory disease have been infrequently described (*1*) and generally emphasize the inflammatory nature of the lesion. The bizarre and pleomorphic astroglial nuclei suggestive of malignancy also occur in inflammatory disease plaques. The most prominent feature of these lesions was monotonous sheets of astroglia, most of which had hypertrophic cell bodies. Large numbers of foamy macrophages in characteristic infiltrative patterns were interspersed evenly among the astroglia and were not associated with necrosis. Small focal collections of inflammatory cells occasionally surround the blood vessels and are sometimes difficult to distinguish from malignant lymphoma.

Patients with a diagnosis confirmed by biopsy do well with steroid and anticonvulsant medication, even in the presence of mass effect, showing progressive regression of the lesion over time together with improvement in clinical status. These patients seem to have a comparatively benign course in comparison with other forms of demyelinating disease and have long periods of remission (*13*).

CONCLUSION

Our 4 patients with clinical and radiologic findings strongly suggestive of malignant glioma were shown by biopsy to have inflammatory demyelinating disease. Such patients illustrate the importance of considering a demyelinating lesion in the differential diagnosis of a similar mass

lesion. The difficulties in establishing the correct diagnosis of inflammatory disease are related to the variations in the radiologic appearance, which require exclusion of malignant gliomas or other brain tumors before the therapeutic strategy can be selected.

REFERENCES

1. Hunter SB, Ballinger WE, Rubin JJ. Multiple sclerosis mimicking primary brain tumor. *Arch Pathol Lab Med.* 1987;111:464–468.
2. Nelson MJ, Miller SL, McLain LW Jr, Gold LH. Case report: multiple sclerosis—large plaque causing mass effect and ring sign. *J Comput Assist Tomogr.* 1981;5:892–894.
3. Nussel F, Wegmuller H, Laseyras F, Posse S, Herschkowitz N, Huber P. Neuro-Becet: acute and sequential aspects by MRI and MRS. *Eur Neurol.* 1991;31: 399–402.
4. Revel MP, Valiente E, Gray F, et al. Concentric MR patterns in multiple sclerosis: report of two cases. *J Neuroradiol.* 1993;20:252–257.
5. Sagar HJ, Warlow CP, Sheldon PW, Esiri MM. Multiple sclerosis with clinical and radiological features of cerebral tumor. *J Neurol Neurosurg Psychiatry.* 1986;45:802–808.
6. Stefano ND, Caramanos Z, Preul MC, Francis G, Antel JP, Arnold DL. In vivo differentiation of astrocytic brain tumors and isolated demyelinating lesions of the type seen in multiple sclerosis using ^{1}H magnetic resonance spectroscopic imaging. *Ann Neurol.* 1998;44:273–278.
7. Arnold DL, Matthews PM, Francis GS. Proton magnetic resonance spectroscopic imaging for metabolic characterization of demyelinating plaques. *Ann Neurol.* 1992;31:235–241.
8. Landtblom AM, Sjoqvist L, Soderfeldt B, Nyland H, Thuomas KA. Proton MR spectroscopy and MR imaging in acute and chronic multiple sclerosis: ringlike appearances in acute plaques. *Acta Radiol.* 1996;37:278–287.
9. Davie CA, Hawkins CP, Barker GJ, et al. Detection of myelin breakdown products by proton magnetic resonance spectroscopy. *Lancet.* 1993;341:630–631.
10. Bitsch A, Bruhn H, Vougioukas V, et al. Inflammatory CNS demyelination: histopathologic correlation with in vivo quantitative proton MR spectroscopy. *AJNR.* 1999;20:1619–1627.
11. Richards TL. Proton MR spectroscopy in multiple sclerosis: value in establishing diagnosis, monitoring progression and evaluating therapy. *AJNR.* 1991;157: 1073–1078.
12. Kumabe T, Shimizu H, Sonoda Y, Shirane R. Thallium-201 single-photon emission computed tomographic and proton magnetic resonance spectroscopic characteristics of intracranial ganglioglioma: three technical case reports. *Neurosurgery.* 1999;45:183–187.
13. Katz D, Taubenberger JK, Cannella B, McFarlin DE, Raine CS, McFarland HF. Correlation between magnetic resonance imaging findings and lesion development in chronic, active multiple sclerosis. *Ann Neurol.* 1993;34:661–669.
14. Shimizu H, Kumabe T, Tominaga T, et al. Noninvasive evaluation of malignancy with proton magnetic resonance spectroscopy in human brain tumors. *AJNR.* 1996;17:737–747.
15. Black KL, Hawkins RA, Kim KT, Becker DP, Lerner C, Marciano D. Use of thallium-201 SPECT to quantitate malignancy grade of gliomas. *J Neurosurg.* 1989;71:342–346.
16. Ishibashi M, Taguchi A, Sugita Y, et al. Thallium-201 in brain tumors: relationship between tumor cell activity in astrocytic tumor and proliferating cell nuclear antigen. *J Nucl Med.* 1995;36:2201–2206.
17. Kaplan WD, Takvorian T, Morris JH, Rumbaugh CL, Connolly BT, Atkins HL. Thallium-201 brain tumor imaging: a comparative study with pathologic correlation. *J Nucl Med.* 1987;28:47–52.
18. Sehweil AM, McKillop JH, Milroy R, Wilson R, Abdel-Dayem HM, Omar YT. Mechanism of ^{201}Tl uptake in tumours. *Eur J Nucl Med.* 1989;15:376–379.
19. Sonoda Y, Kumabe T, Takahashi T, Shirane R, Yoshimoto T. Clinical usefulness of ^{11}C-MET PET and ^{201}Tl SPECT for differentiation of recurrent glioma from radiation necrosis. *Neurol Med Chir (Tokyo).* 1998;38:342–348.
20. Kondo T, Kumabe T, Maruoka S, Yoshimoto T. Diagnostic value of ^{201}Tl-single-photon emission computerized tomography studies in cases of posterior fossa hemangioblastomas. *J Neurosurg.* 2001;95:292–297.